

# Conformational flexibility of ribosomal decoding-site RNA monitored by fluorescent pteridine base analogues

Jerod Parsons and Thomas Hermann\*

Department of Chemistry and Biochemistry, University of California, San Diego, 9500 Gilman Drive, La Jolla, CA 92093, United States

Received 14 August 2006; revised 24 August 2006; accepted 24 August 2006  
Available online 3 February 2007

**Abstract**—Conformational transitions in ribosomal decoding-site RNA have previously been monitored by replacement of flexible adenine bases with fluorescent 2-aminopurine (2AP). Here, we have studied pteridine base analogues 3-methylisoxanthopterin (3MI) and 6-methylisoxanthopterin (6MI) as fluorescent labels for the investigation of conformational changes in the decoding site that are triggered by ligand binding. The higher quantum yield of 3MI and 6MI along with their relatively red-shifted excitation and emission wavelengths renders the pteridines interesting alternatives to 2AP for the establishment of ligand-binding assays for RNA based on fluorescence labelling.  
© 2007 Elsevier Ltd. All rights reserved.

## 1. Introduction

The decoding site within 16S ribosomal RNA (rRNA) in the 30S subunit provides the mechanism by which the protein synthesis machinery deciphers the genetic code of messenger RNA (mRNA). Correspondence between the mRNA codon and the anticodon of the aminoacylated transfer RNA (tRNA) is monitored by direct interaction with conformationally flexible adenine bases 1492 and 1493 within an internal RNA loop of the decoding site (Fig. 1). The decoding process involves a transition between distinct conformational states of A1492 and A1493 that projects both bases away from the interior of the rRNA helix and

towards the ribosomal mRNA binding cleft where they contact directly the codon–anticodon hybrid.<sup>1</sup> The decoding-site loop is the target for aminoglycoside antibiotics (Fig. 2), which kill bacteria by reducing the decoding fidelity of the ribosome. The mechanism of action of the aminoglycosides has been linked to their ability to bind specifically to the bacterial decoding-site loop and thereby lock the conformation of adenines 1492 and 1493 in a state that impedes discrimination between cognate and near-cognate tRNA–mRNA complexes.<sup>2,3</sup>

Conformational transitions in the decoding site and the impact of ligand binding have been studied by NMR, X-ray crystallography and fluorescence labelling. The ribosomal decoding-site RNA is uniquely suitable for such investigations as it can be isolated from the ribosomal

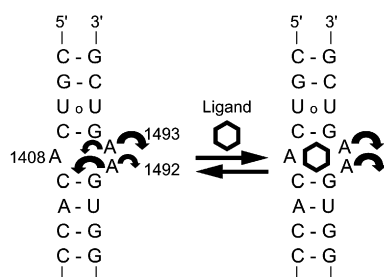


**Figure 1.** The bacterial decoding-site RNA contains two flexible adenines (A1492, A1493) which, in the absence of bound ligand, sample conformational space in the interior and outside the RNA helix. Binding of specific ligands, including aminoglycoside antibiotics, stabilizes a conformation with both adenine residues projected away from the helix and into the solvent. The ligand-induced transition can be monitored by replacing either of the adenines with a fluorescent base analogue.

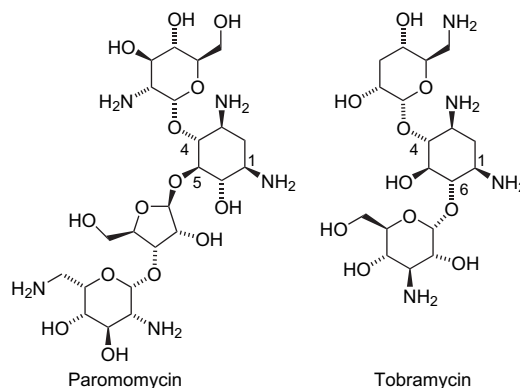


**Figure 2.** Structures of aminoglycoside antibiotics that bind to the bacterial decoding-site RNA.

\* Corresponding author. Tel.: +1 858 534 4467; fax: +1 858 534 0202; e-mail: tch@ucsd.edu

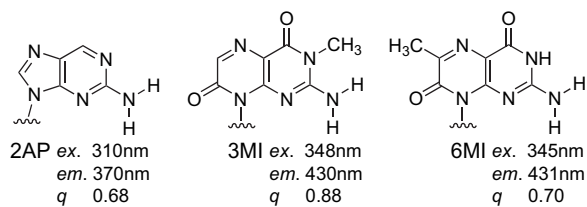


**Figure 3.** Structures of fluorescent nucleobase analogues, 2-aminopurine (2AP), 3-methylisoxanthopterin (3MI) and 6-methylisoxanthopterin (6MI), along with their excitation and emission wavelengths.

context and inserted into model oligonucleotides that retain the dynamic and ligand-binding characteristics of the rRNA.<sup>4</sup>

Previously, 2-aminopurine (2AP) has been used to replace adenines at the positions 1492 and 1493 to obtain fluorescently labelled decoding-site RNA for ligand-binding studies (Fig. 3).<sup>5,6</sup> While the 2AP nucleoside has a high quantum yield (0.68) at neutral pH and a low excitation energy as compared to the natural nucleosides and can therefore be selectively excited,<sup>7</sup> incorporation into oligonucleotides reduces its fluorescence quantum yield up to 100-fold, requiring thus high concentrations of 2AP-labelled oligonucleotides. Moreover, 2AP has relatively short-wavelength excitation and emission maxima, which potentially interfere with absorption by aromatic ligands in binding studies of the decoding-site RNA. To overcome the limitations of 2AP, we studied fluorescence labelling of the bacterial decoding site with the pteridine base analogues 3-methylisoxanthopterin (3MI) and 6-methylisoxanthopterin (6MI), which have more favourable photophysical properties,<sup>8</sup> yet bear less structural resemblance to the natural nucleoside bases (Fig. 3). Applications of the pteridine base analogues for studying DNA structure have been reviewed before.<sup>9</sup>

## 2. Results and discussion

To study interactions of fluorescently labelled decoding-site RNA with aminoglycosides we used a previously established oligonucleotide model of the bacterial target (Fig. 4).<sup>5</sup> The adenine at position 1493 was replaced by either 2AP, 6MI, or 3MI. Titrations of the labelled oligonucleotide were performed with tobramycin and paromomycin as

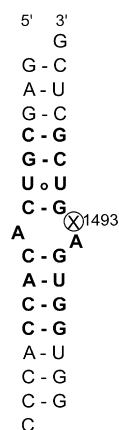


**Figure 4.** Secondary structure of the decoding-site oligonucleotide used for titrations. The adenine at position 1493 (X) was replaced by the fluorescent bases 2AP, 6MI, or 3MI.

representatives of, respectively, the 4,6- and 4,5-substituted 2-deoxystreptomycin aminoglycosides (Fig. 2). It had been shown earlier that binding of these aminoglycosides to 2AP(1493)-labelled decoding site leads to a dose-dependent decrease of fluorescence due to displacement of adenine 1492 from the RNA interior and stacking of this base on the fluorescent label at position 1493.<sup>5,6</sup>

Control titrations of the 2AP-labelled oligonucleotide showed the expected dose response (Fig. 5). Apparent binding affinities ( $EC_{50}$ ) calculated from fitting of dose–response curves to the 2AP titrations were consistent with relative  $K_D$  values previously reported for tobramycin and paromomycin (Table 1).<sup>5,6</sup> Titrations of pteridine-labelled oligonucleotides with aminoglycosides revealed fluorescence responses that were distinct for both the aminoglycoside class (tobramycin or paromomycin) and label (6MI or 3MI) (Fig. 5). Overall, tobramycin induced a similar dose-dependent quenching of fluorescence in both 6MI- and 3MI-labelled oligonucleotides. In contrast to the 2AP titration, a biphasic response was observed for the pteridine labels, which showed a slight increase of fluorescence upon addition of tobramycin, before quenching occurred. The biphasic behaviour suggests detection of secondary binding events that are not observed or not present for the 2AP label. Tobramycin binding reduced fluorescence of the pteridine-labelled RNA by about 30% while quenching of the 2AP label amounted to 50%.  $EC_{50}$  values calculated for the fluorescence decrease induced by tobramycin addition to the 6MI- and 3MI-labelled oligonucleotides were about 2-fold higher than those observed for the 2AP label but consistent within the pteridines (1.8–1.9  $\mu$ M, Table 1).

Unlike for tobramycin, fluorescence responses of the pteridine-labelled oligonucleotides to paromomycin were inconsistent. The 6MI label showed quenching upon paromomycin addition with a total reduction of the signal by about 30%, comparable to the tobramycin experiments with 6MI. However, the  $EC_{50}$  value of paromomycin binding was roughly 6-fold higher for the 6MI label compared to 2AP. Surprisingly, the 3MI-labelled oligonucleotide showed a slight increase in fluorescence ( $\sim$ 10%) upon titration with paromomycin but no dose-dependent quenching as would be expected from aminoglycoside binding.

To investigate the impact of the pteridine fluorescent labels on the structural stability of the decoding-site oligonucleotide relative to the 2AP-labelled RNA, we recorded thermal denaturation ('melting') profiles by measuring UV absorption at 260 nm (Fig. 6). Melting curves were recorded for the decoding-site RNA in the free form and in the presence of either 1 mM magnesium ion or 1 mM magnesium and 1 mM aminoglycoside (paromomycin) combined.

As expected, the presence of magnesium led to a large up-shift of the denaturation temperature for all three constructs (2AP-, 6MI- and 3MI-labelled, Fig. 6), reflecting stabilization of the RNA by metal ion binding. Addition of aminoglycoside caused minimal further stabilization, consistently observed in all three constructs. Interestingly, the melting curves were virtually identical for the three distinctly labelled constructs in the presence of either magnesium alone or magnesium and aminoglycoside, while stability

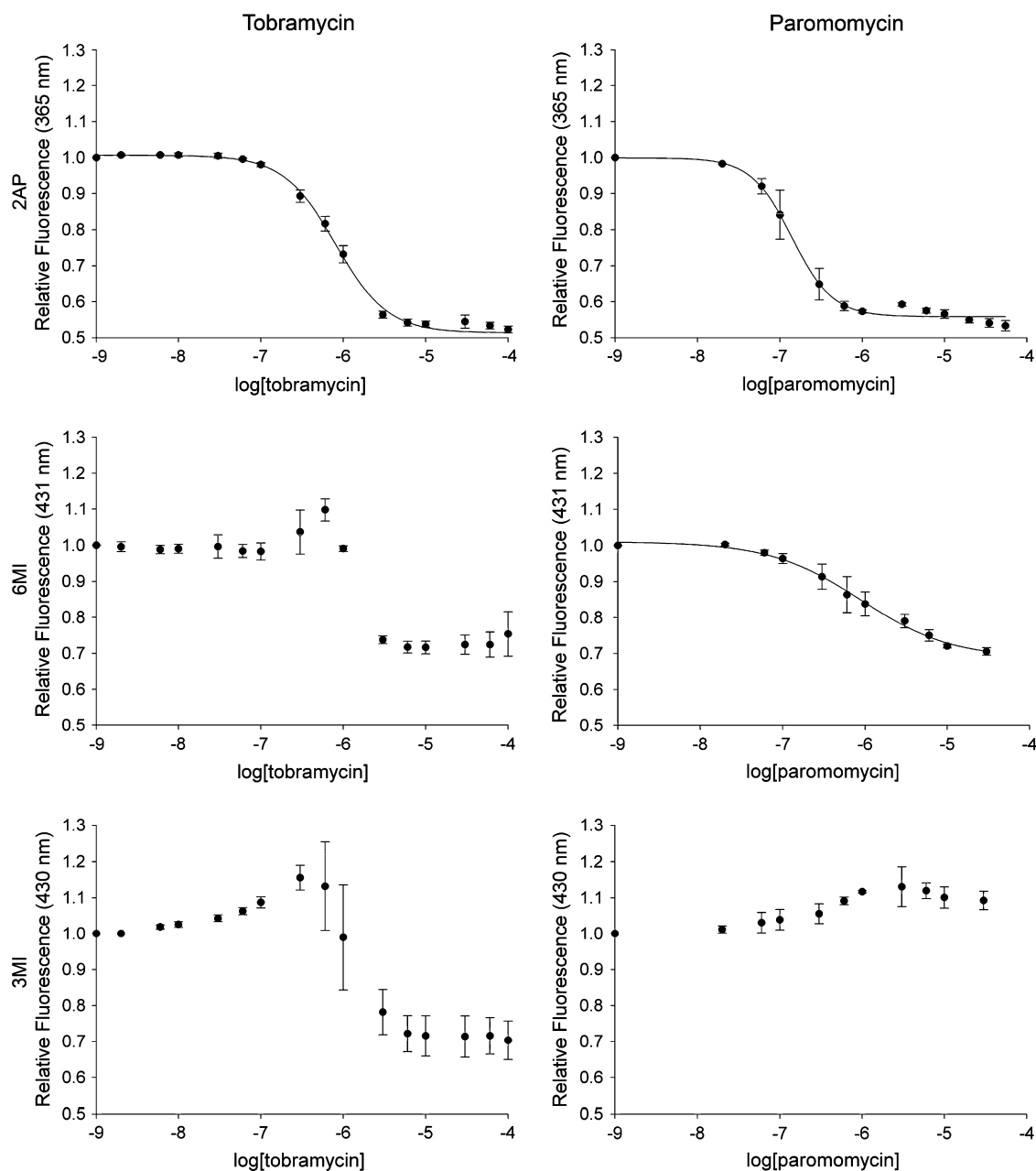


**Figure 5.** Titrations of fluorescently labelled decoding-site oligonucleotide with tobramycin and paromomycin. Data points are averages of three experiments with error bars indicating  $\pm\sigma$ .

differences were seen for the free RNAs (Fig. 6). Both pteridine-labelled RNAs showed a slightly lower thermal stability ( $\sim 2^\circ\text{C}$ ) compared to the 2AP construct. These findings suggest that interactions of the 2AP base that stabilize the strands of the decoding-site RNA, perhaps by cross-strand contacts with A1408 (see Fig. 1), might not be present in

**Table 1.**  $\text{EC}_{50}$  values ( $\mu\text{M}$ ) determined from titration curves of fluorescently labelled decoding-site oligonucleotide with aminoglycosides (see Fig. 5)

X=	Tobramycin	Paromomycin
2AP	$0.81 \pm 0.09$	$0.14 \pm 0.03$
6MI	$1.8 \pm 1.1$	$0.89 \pm 0.71$
3MI	$1.9 \pm 0.7$	n.d.

In case of biphasic titration curves (3MI and 6MI), values were calculated for fluorescence quenching.

the pteridine-labelled RNAs. The identical denaturation behaviour of the three labelled RNAs in the presence of magnesium or magnesium and aminoglycoside suggests that metal ion and drug binding stabilize a structure of the decoding site that does not involve the base at position 1493. In other words, the nature of the fluorescent label at this position does not affect formation of the metal ion and aminoglycoside complexes, in agreement with previous studies of 2AP-labelled decoding-site constructs.<sup>5,6</sup>

### 3. Conclusions

Aminoglycoside titrations of decoding-site oligonucleotides show that fluorescent pteridine base analogues 6MI and 3MI can be used in lieu of 2AP to monitor conformational

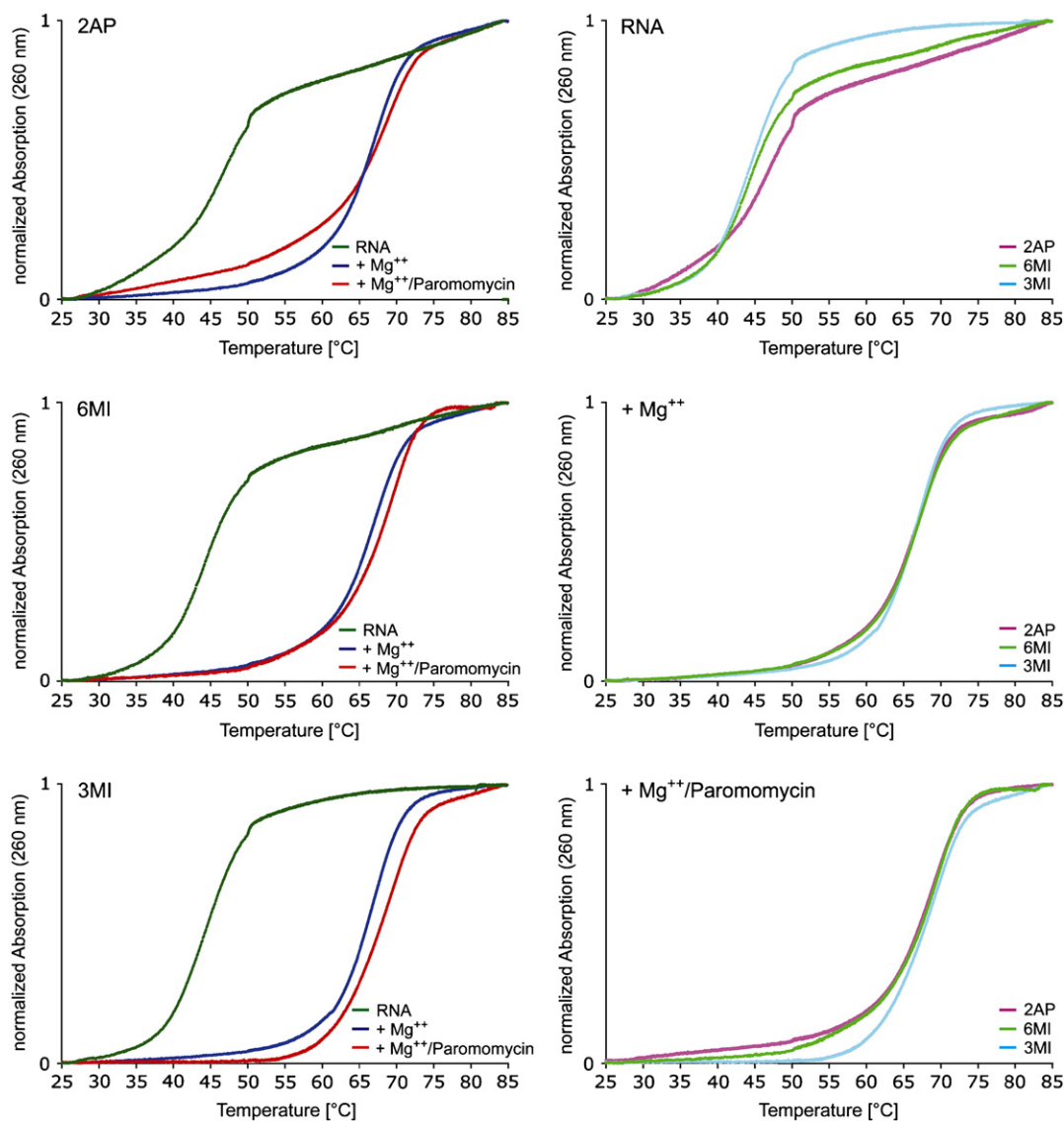


**Figure 6.** Melting profiles determined by UV absorption at 260 nm for fluorescently labelled decoding-site oligonucleotides. Left: profiles for the three different labels (2AP, 6MI, 3MI) for RNA alone (green) and in the presence of 1 mM magnesium chloride (blue) as well as 1 mM magnesium chloride together with 1 mM paromomycin (red). Right: comparison of the three labelled RNAs for the three different conditions (RNA, RNA/1 mM magnesium chloride, RNA/1 mM magnesium chloride/1 mM paromomycin).

changes triggered by ligand binding to the RNA target. In contrast to 2AP, which is structurally very similar to adenine, the pteridine analogues share less structural resemblance with purine bases. While 2AP had previously been shown to be a universally responsive fluorescent label for the monitoring of ligand binding to the decoding-site RNA, the pteridine analogues revealed a more idiosyncratic behaviour dependent on the type of label (6MI or 3MI) and aminoglycoside (4,5- or 4,6-disubstituted 2-DOS derivatives). For example, titration of a bonafide high-affinity ligand (paromomycin) with 3MI-labelled decoding-site RNA did not elicit the expected change in fluorescence intensity. Secondary binding events complicate the deconvolution of fluorescence titration curves. The behaviour of the pteridine labels might in part be dependent on the site of incorporation within the RNA. For the decoding site, the 1493-position might not be optimal for labelling with 3MI or 6MI. Therefore, while the photophysical properties of the pteridine analogues render them useful as fluorescent labels for affinity

screening of RNA, careful validation of pteridine-labelled constructs is required by using known ligands and 2AP-labelling as a reference. Thermal denaturation studies of labelled decoding-site constructs in the presence of magnesium ions and aminoglycoside suggest that the nature of the fluorescent label (2AP or pteridine) does not affect the stability of the RNA-drug complexes while denaturation of the free RNA might depend on interactions of the fluorescent modified base.

## 4. Experimental

### 4.1. RNA and aminoglycosides

RNA was purchased from Dharmacon Research (Lafayette, CO) (unlabelled and 2AP-labelled RNA) and Trilink Biotechnologies (San Diego, CA) (6MI- and 3MI-labelled RNA). Oligonucleotides were purified by gel electrophoresis,

transferred to 10 mM sodium cacodylate buffer, pH 6.5, and annealed by heating to 75 °C followed by snap cooling on ice. Aminoglycosides were purchased as sulfates from RPI (Mt. Prospect, IL) and used without further purification.

#### 4.2. Fluorescence spectroscopy

Fluorescence measurements were performed on a thermostatted RF-5301PC spectrofluorometer (Shimadzu, Columbia, MD) at 25 °C. Emission spectra were recorded in 10 mM sodium cacodylate buffer, pH 6.5, at 0.5 μM RNA concentration and while irradiating at 310 nm (2AP), 345 nm (6MI), or 348 nm (3MI). EC<sub>50</sub> values were calculated with the Sigmaplot software (Systat Software, Point Richmond, CA) by fitting a dose–response curve to the normalized fluorescence intensity plotted versus the log of aminoglycoside concentration. Normalized relative fluorescence (Fig. 5) was calculated by subtracting background signal measured in a titration of compound into buffer and normalization by the fluorescence intensity of the labelled free RNA.

#### 4.3. UV absorption spectroscopy

UV melting experiments were performed on a thermostatted UV-2401PC spectrofluorometer (Shimadzu, Columbia, MD). RNA at 1.5 μM concentration in 10 mM sodium cacodylate buffer, pH 6.5, was heated from 25 to 85 °C at a rate of 0.25 °C/min. Depending on the experiment, 1 mM MgCl<sub>2</sub> or

1 mM MgCl<sub>2</sub> and 1 mM aminoglycoside were present. RNA samples were covered with a thin layer of silicone oil to prevent evaporation during heating. Absorption was recorded at 260 nm every 6 s.

#### Acknowledgements

This work was supported by faculty startup funds from the University of California, San Diego.

#### References and notes

1. Ogle, J. M.; Ramakrishnan, V. *Annu. Rev. Biochem.* **2005**, *74*, 129–177.
2. Ogle, J. M.; Brodersen, D. E.; Clemons, W. M., Jr.; Tarry, M. J.; Carter, A. P.; Ramakrishnan, V. *Science* **2001**, *292*, 897–902.
3. Vicens, Q.; Westhof, E. *ChemBioChem* **2003**, *4*, 1018–1023.
4. Hermann, T. *Biochimie* **2006**, *88*, 1021–1026.
5. Shandrick, S.; Zhao, Q.; Han, Q.; Ayida, B. K.; Takahashi, M.; Winters, G. C.; Simonsen, K. B.; Vourloumis, D.; Hermann, T. *Angew. Chem., Int. Ed.* **2004**, *43*, 3177–3182.
6. Kaul, M.; Barbieri, C. M.; Pilch, D. S. *J. Am. Chem. Soc.* **2004**, *126*, 3447–3453.
7. Ward, D. C.; Reich, E.; Stryer, L. *J. Biol. Chem.* **1969**, *244*, 1228–1237.
8. Driscoll, S. L.; Hawkins, M. E.; Balis, F. M.; Pfeleiderer, W.; Laws, W. R. *Biophys. J.* **1997**, *73*, 3277–3286.
9. Hawkins, M. E. *Cell Biochem. Biophys.* **2001**, *34*, 257–281.